IEEE Access
Multidisciplinary | Rapid Review | Open Access Journal

Received July 8, 2019, accepted July 26, 2019, date of publication August 6, 2019, date of current version August 20, 2019.

Digital Object Identifier 10.1109/ACCESS.2019.2933404

High Gain and Low Grating Lobe Electrically Large Array Antenna by Using Fabry-Perot Cavity

YUNYANG ZHANG[1], WENQUAN CAO[1,2], ZUPING QIAN[1], AND TING PAN[1]
[1]College of Communications Engineering, Army Engineering University of PLA, Nanjing 210007, China
[2]State Key Laboratory of Millimeter Waves, Southeast University, Nanjing 210096, China

Corresponding author: Wenquan Cao (cao_wenquan@163.com)

This work was supported in part by the National Natural Science Foundation of China under Grant 61871399 and Grant 61401506, in part by the China Postdoctoral Science Foundation under Grant 2016M600349 and Grant 2017T100316, and in part by the Jiangsu Province Natural Science Foundation under Grant BK20160080.

ABSTRACT In this paper, a high gain and low grating lobe electrically large array antenna is proposed by using Fabry-Perot cavity (FPC). The feeding array antenna is composed by elements with electrically large property (ELP) based on TM_{30} mode. The FPC between a ground plane and a single-layer partially reflecting surface (PRS) made by substrate with arrays of square metal patches printed on both the top and bottom surfaces is used here to narrow the beamwidth of element patterns, thus the large grating lobes of array caused by large element spacing can be avoided. By analyzing the parameters of PRS unit cell, suitable cell spacing is determined. Finally, a 2×2 array was fabricated and measured to validate its effectiveness. Measurements demonstrate that the gain of the array can reach up 20.9dBi at the center working frequency. When the element spacing is $1.47\lambda_0$, the maximum grating lobe level at 21GHz is only -15.5dB.

INDEX TERMS High gain, low grating lobe, electrically large property (ELP), TM_{30} mode, Fabry–Perot cavity (FPC).

I. INTRODUCTION

Microstrip antenna plays an important role in communication system. With the actual requirements of broadband and high-speed data transmissions, the development of microstrip components in millimeter wave (MMW) and terahertz (THz) wave bands have become an inevitable trend. However, the fabrication accuracy of MMW and THz wave antennas will soon reach micron level as the operating frequency increases, which requires greater demands on machining precision and fixed installation of some equipment. Planar antennas with electrically large property (ELP) that break through size limitation of traditional patch antenna can solve the problem to some extent [1]–[3]. Nevertheless, it is difficult to design array antenna with ELP according to the array theory. As we know, the elemental periodic intervals of array are usually less than $1\lambda_0$. Since the particular size of the ELP antenna is usually more than one wavelength, the element spacing of ELP array is greater than one wavelength consequentially and undesirable larger side lobes or even grating lobes will appear in the array patterns inevitably.

Facing the confine mentioned above, some methods have been proposed. One of typical strategies is adopting random distribution of subarrays or elements. By disrupting distribution, the grating lobes of subarrays will not overlap in-phase or have different angular directions, which avoids large grating lobes appeared in array patterns [4]–[8]. According to the models proposed in [5] and [6], by considering multiple arrays such as periodic subarrays, unequally spaced subarrays and phased subarrays etc., the grating lobes level can be reduced by 2.6dB∼11dB. Similarly, optimized amplitude weighting, random subarray and random staggering of the rows were also be used to suppress grating lobes in [8] and the levels can be reduced to -3.77dB∼ -20dB. However, these typological methods are usually based on special optimization algorithms and salient number of subarrays or elements, which will dramatically increases complexity of optimization and fabrication. Different from the previous method, tactics of making the null/(zero) ranges of element pattern coincide with the grating lobes of array factor (AF) can considerably

The associate editor coordinating the review of this manuscript and approving it for publication was Kuang Zhang.

decreases complexity of design and optimization as well as simplify manufacturing and reduce cost. This method of solving large element spacing in arrays is proposed and applied in [9]. When the element spacing is more than $1.4\lambda_0$, the grating lobes level are lower than -22dB. What should be emphasized is that the second approach also has application conditions. If element patterns of E-plane and H-plane do not have null/(zero) ranges concurrently, it will be difficult to apply this method to a 2-D array antenna. Namely, if the beamwidth of E-plane and H-plane can be narrowed simultaneously and the high level regions of element pattern can be avoided by grating lobes of AF, the influence caused by large element spacing in 2-D arrays can also be reduced.

As is well-known, Fabry-Perot cavities (FPC) is often used to enhance antenna gain and expand bandwidth [10]–[18] compared with traditional antennas [19], [20]. Actually, this structure also has excellent advantage to suppress the grating lobes of array caused by large element spacing. However, there is little specific research on it. As described in [10], an FPC with artificial magnetic conductor (AMC) walls is adopted to suppress grating lobe of array with $2\lambda_0$ element spacing. But this work is only implemented in 1-D array antenna and the height of the AMC wall is higher. Similarly, by introducing PRS on the top of feeding antenna in [11], the grating lobes of array with $2\lambda_0$ element spacing can be controlled lower than -7dB. But the above work only considered the gain and polarization performance but ignored the element spacing. Thus the grating lobe level is relatively high.

In this paper, a high gain and low grating lobe electrically large array antenna by using FPC is proposed. Since the beamwidth of the antenna patterns can be narrowed by loading partially reflecting surface (PRS) above the feeding antenna, it can be applied to design low grating lobe array antennas with ELP. Section II analyzes the performance of the PRS unit cell with different parameters and the influence of PRS on beamwidth of element antenna. Array theory and parameters selection are discussed in Section III. What's more, one 2×2 array is fabricated for verification and Section III also gives the simulated and measured results. Finally, conclusion is made in Section IV.

II. ANTENNA DESIGN AND WORKING PRINCIPLE

The antenna element of array is discussed in this section. Properties of the PRS unit cell are analyzed and influences of PRS on the ELP feeding element pattern are also described in details.

A. GEOMETRY OF ANTENNA ELEMENT

Fig. 1(a) describes the overall structure of the antenna element, which consists of a feeding antenna with ELP and a single-layer metallic PRS. Both the feeding antenna and PRS are designed based on the material of DiClad 880 (permittivity: 2.2) with thickness of $h_1 = 0.5$mm. In Fig. 1(d) and 1(e), the feeding antenna is composed of a square patch surrounded by substrate integrated waveguide (SIW) and a

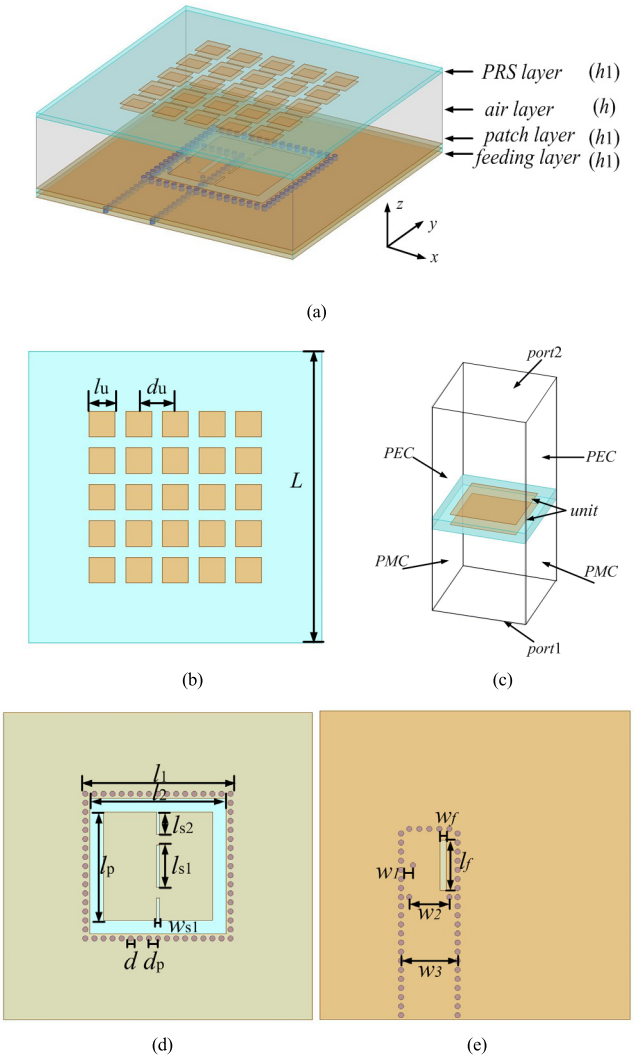

FIGURE 1. Geometry of the proposed antenna. (a) Overall view, (b) top view of PRS, (c) explode view of the PRS unit cell, (d) top view of the ELP feeding patch, (e) top view of the feeding network.

single-layer SIW feeding network. The resonant mode of the patch is TM_{30}. According to the principle described in [21], [22], by introducing a rectangular slot along the central line of patch, the reverse phase current of the high-order mode can be destroyed and the side lobes can be effectively reduced. Furthermore, by installing two slots on the non-radiating edge of the patch, the beamwidth of H-plane can also be narrowed. Although the feeding antenna has the properties of high gain and ELP, it is difficult to be used in ELP arrays. Different from the traditional half-wavelength resonant antenna, due to the size of ELP antenna is larger than one wavelength, the element spacing of array must be over than $1\lambda_0$. From descriptions in Section I, undesirable large side lobes or even grating lobes appears in the array patterns.

In order to solve the above contradiction and realize low grating lobe array by using ELP element, in Fig. 1(b), a single-layer PRS is added as a superstrate above the ELP antenna to adjust the element patterns. According to the ray

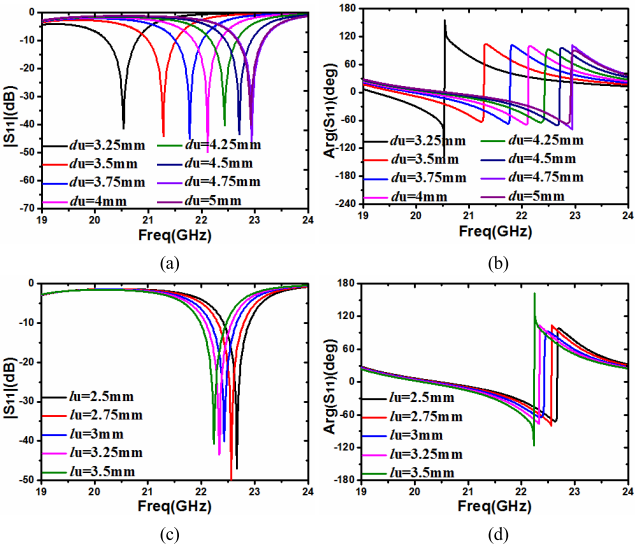

FIGURE 2. Simulated complex reflection coefficient with different parameters. (a) Amplitude for varying d_u, (b) phase for varying d_u, (c) amplitude for varying l_u, (d) phase for varying l_u.

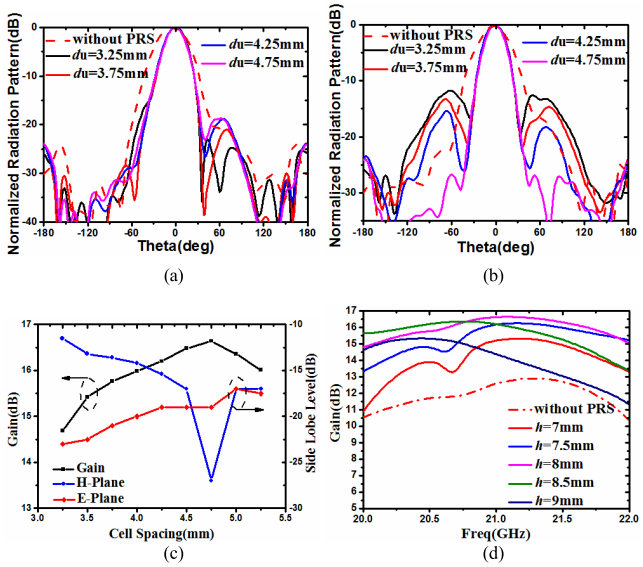

FIGURE 3. The radiation patterns and gains of element with different conditions. (a) The E-plane with varying d_u, (b) the H-plane with varying d_u, (c) the relationship between cell spacing (d_u) and gain and side lobes level, (d) the relationship between gain and height of air-layer (h).

optics model, the relation between the maximum directivity ($D_{\max}$) of the FPC antenna and the complex reflection coefficient ($Re^{j\varphi \mathrm{prs}}$) of the PRS layer can be expressed as

$$D\max = \frac{1 + \left|Re^{j\varphi_{prs}}\right|}{1 - \left|Re^{j\varphi_{prs}}\right|} \tag{1}$$

The thickness of the FPC (h) is given by

$$-\pi + \varphi_{\mathrm{prs}} - 4\pi h/\lambda_0 = 2N\pi, \quad N = 0, \pm 1, \pm 2, \ldots \tag{2}$$

where $-\pi$, φ_{prs} and λ_0 are the reflection phase of ground plane, the reflection phase of PRS and the operating wavelength in free space, respectively. As can be observed from (1), it reveals that larger reflection coefficient leads to higher directivity. Usually, the reflection phase φ_{prs} of a highly reflective PRS is about $-\pi$ and thus the minimum h is about $\lambda_0/2$.

B. PARAMETER ANALYSIS

The PRS layer is made by single-layer with arrays of metal square patches printed both on top and bottom surfaces. The performances of the feeding antenna with ELP are highly relevant with the properties of the PRS layer. Thus the first work is analyzing the unit cell of the PRS layer. The boundary conditions of electric and magnetic walls and the two ports of waveguide are described in Fig. 1(c). Since the unit cell is two symmetric squares structure, both horizontally polarized wave and vertically polarized wave will show similar performance.

Reflection magnitude and phase of the unit cell for different periodic spacing are shown in Fig. 2(a) and 2(b). With the increase of d_u, the resonant point transforms to higher band. What's more, it also can be seen that, at the operating frequency $f_0 = 21$GHz, the reflection magnitude become stronger and the reflection phase is much gentler. Meanwhile, when the value of d_u is greater than 1.25mm, the changes of reflection magnitude are not significant. These results indicate that with the increase of the cell spacing, the performance of the element will be enhanced.

Furthermore, by adjusting the size of unit (l_u), the reflection magnitude and phase will also be changed. With the decrease of the value of l_u, the resonant point also transforms to higher band in Fig. 2(c) and 2(d). However, the changes are not evident compared with the periodic spacing of the PRS unit cell.

The element patterns of E-plane and H-plane are exhibited in Fig. 3(a) and 3(b). The red dotted lines are the patterns of the feeding antenna and the −15dB beamwidth is about 100°. By added a single-layer PRS above the feeding antenna, the beamwidth is narrowed obviously by 50°. Due to the beamwidth of element pattern is narrowed, which provides a favorable conditions for the grating lobes of AF to avoid the high level regions of element pattern. At that time, with the increase of PRS unit cell distance, side lobes of H-plane will become smaller and smaller. Although the side lobes of E-plane are increased, the levels are always less than -15dB. What's more, the changes of E-plane are not dramatically compared with the H-plane. Fig. 3(c) directly expresses the relationship of the values of d_u, antenna gain and side lobe level, which is highly consistent with the previous analysis results of the PRS unit cell. With the expansion of the cell spacing, the reflection wave in the cavity becomes more symmetrical, and the energy of the side lobes converges to the main lobe gradually. As can be seen from Fig. 3(c), when the element spacing is 1.75mm, the element gain will reach the maximum value and the element has good performance and lowest side lobes.

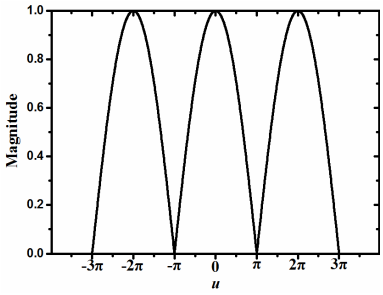

FIGURE 4. The array factor of 2 × 2 equidistant array.

Meanwhile, since the resonant frequency is 21GHz, the height of the air-filled layer (h) is 7.14mm by using the equation (2). However, it should be noticed that the above ray optics model is only a reference principle and the actual parameters still need to be optimized according to the proposed model. From the Fig. 3(d), by adjusting the value of h, the maximum gain is obtained at $h = 8$mm. Compared with the element without PRS, the gain of the proposed antenna can be enhanced about 4dB.

III. FABRICATION AND MEASUREMENT RESULTS OF 2 × 2 ARRAY ANTENNA

Based on the array theory, a suitable antenna element is selected in this section and a 2 × 2 array is fabricated and measured.

A. SELECTED ELEMENT OF ARRAY

According to the array theory, the array patterns are multiplied by the element patterns and AF

$$F(\theta) = F_1 \cdot F_a \tag{3}$$

where $F(\theta)$, F_1 and F_a are array patterns, element patterns and AF respectively. As for a $N \times N$ array ($N = 2, 3, 4\ldots$), the amplitude of the individual elements are assumed equal. As an example, F_a of 2 × 2 array can be expressed as the following equation

$$Fa = Fx \cdot Fy = \frac{\sin\frac{Nu_x}{2}}{N\sin\frac{u_x}{2}} \cdot \frac{\sin\frac{Nu_y}{2}}{N\sin\frac{u_y}{2}} \tag{4}$$

$$u_x = -kd_x + \varphi_x \sim kd_x + \varphi_x \tag{5}$$

$$u_y = -kd_y + \varphi_y \sim kd_y + \varphi_y \tag{6}$$

where d_x (d_y) and k are the separation distance between individual elements and the free space wave number. The parameter φ_x (φ_y) is the phase of the individual elements. For array antennas with the same phase, the value of φ_x (φ_y) is 0.

In order to determine the suitable element for array, the first step is analyzing AF. For the 2 × 2 array with equal spacing and phase, F_x and F_y will have the same results. The pattern of F_x (F_y) can be given in Fig. 4. According to relationship (5) or (6), when the element spacing is λ_0, the value range of u_x or u_y is extended to -2π to 2π, and the visible area will contain three lobes with the same level. Consequently

TABLE 1. Parameters for the proposed antenna element. (Unit: mm).

Symbol	Value	Symbol	Value	Symbol	Value
L	34	l_u	3	d_u	4.25
l_1	16.6	l_2	15	l_p	12
l_{s1}	4.7	l_{s2}	2.5	w_{s1}	0.3
d	0.6	d_p	1	l_f	5.5
w_f	0.7	w_1	0.5	w_2	4.6
w_3	6.2	h	8	h_1	0.5

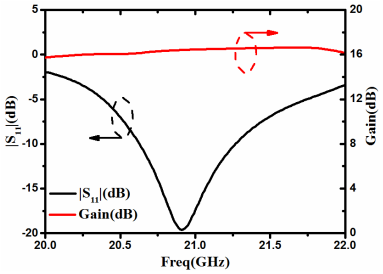

FIGURE 5. The simulated bandwidth and gain of the proposed element.

undesired grating lobes may be created in the array patterns. In order to avoid grating lobes appeared in array patterns, the maximum element spacing may be written as

$$d < \frac{\lambda}{1 + |\cos\theta M|} \tag{7}$$

When the maximum radiation direction is 90° ($\theta_M = 90°$), $d < \lambda_0$ is the significant condition to avoid grating lobes.

Nevertheless, if the grating lobes of the AF can be avoided by the high level ranges of element patterns, the grating lobes of array patterns can be reduced. So the second step is considering the relationship between element spacing and the angle point of grating lobes as shown equation (8).

$$\theta_i = \arccos\left[\frac{1}{kd}(-\varphi \pm 2i\pi)\right] \tag{8}$$

where $i = 0, 1, 2, 3, \ldots i = 0$ express the main lobe and others are grating lobes.

From the analysis in the previous section, although the element has good properties of high gain and low side lobes when the value of d_u is 1.75mm, this is not the main purpose of realizing low grating lobe array with ELP. Because when the unit cell spacing of PRS is 1.75mm, the element spacing of array will reach up $1.8\lambda_0$. According to equation (8), the first grating lobes of the AF will appear at about 37°. As can be seen from the Fig. 6, the first grating lobes of the AF will be superimposed with the high level regions of elements and larger grating lobes will be formed. In order to realize array with ELP, low grating lobes and high gain, the unit cell spacing of PRS should be selected at 1.25mm. The maximum gain of the element is 16.3dB and the maximum side lobe level is low than −15dB. The optimized parameters of the antenna are given in Table 1. The simulated gain and $|S_{11}|$

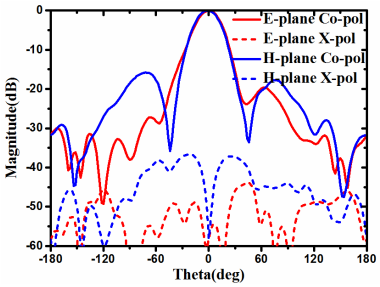

FIGURE 6. Simulated radiation patterns of the proposed element at 21GHz.

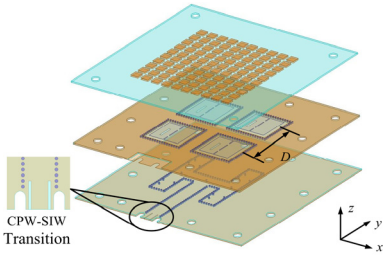

FIGURE 7. Geometry of the proposed 2 × 2 equidistant array.

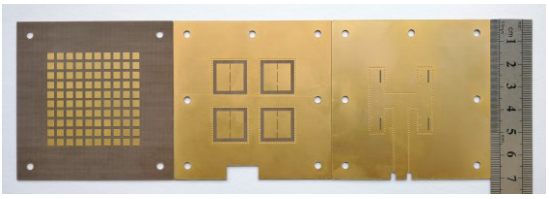

(a)

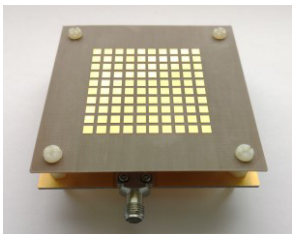

(b)

FIGURE 8. The fabricated 2 × 2 equidistant array.

(20.6 GHz to 21.3GHz) of the proposed antenna element are given in Fig. 5. The radiation patterns of 21GHz are shown in Fig. 6.

B. ARRAY CONFIGURATION AND PERFORMANCES

Based on the antenna element proposed above, a high gain low grating lobes 2×2 array with ELP is fabricated and measured. The model is shown in Fig. 7. The low grating lobe array is composed of a single-layer SIW feeding network, four uniform square patch elements and PRS. It should be noticed that the element spacing (D) is reaching up $1.47\lambda_0$.

Fig. 8 shows the overall prototype of the fabricated array and the ET-launch SMA probe-to-coaxial adaptor is adopted for measurement. The simulated and measured results of

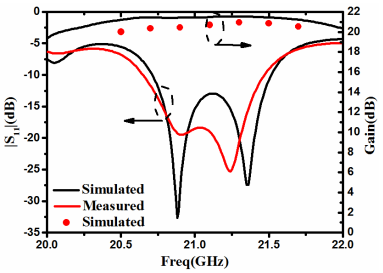

FIGURE 9. The measured and simulated $|S_{11}|$ and gain of the fabricated 2 × 2 array.

TABLE 2. Comparison between proposed antenna and other works.

Ref	Type	Element Number	Gain (dBi)	Element Spacing	GLL (dB)
7	Tradition	16	N/A	$<1.5\lambda_0$	-10
8	Tradition	768	N/A	$<1.36\lambda_0$	-13
9	Tradition-ELP	1/8	13/19	$1.4\lambda_0$	-22
19	Tradition	1/16	6.48/19.1	N/A	N/A
20	Tradition	1/16	6.5/17.8	N/A	N/A
Our work	**FPC-ELP**	**1/4**	**16.3/20.9**	**$1.47\lambda_0$**	**-15.5**
11	FPC	1	13.8	N/A	N/A
12	FPC	2	15.1	N/A	N/A
13	FPC	1/4	12.4/17.2	$2\lambda_0$	-7

gain and $|S_{11}|$ are shown in Fig. 9. It can be found that the measured gain and $|S_{11}|$ are consistent with simulated ones. The impedance bandwidth is 4.3% (20.6 GHz to 21.5GHz). The actual gain reaches up to 20.9 dBi at 21GHz. E-plane and H-plane radiation patterns of the proposed array are shown in Fig. 10(a) and Fig. 10(b), respectively. It can be seen that the maximum grating lobe level is lower than −15.5dB.

C. COMPARISON

Fig. 10(c) and Fig. 10(d) present the result of 2 × 2 array antenna without PRS. Because the element spacing of array is over than $1\lambda_0$ and the beamwidth of element without PRS is wider than the loaded one, thus the maximum grating lobe level are higher than −7dB. Obviously, the grating lobe level of array in Fig. 10(a) and Fig. 10(b) will have little effect on the array performance compared with Fig. 10(c) and Fig. 10(d). This comparison shows that the issue of ELP arrays caused by large element spacing can be effectively solved by using FPC structure.

For further comparison, Table 2 lists the differences between our work and others. Compared with the traditional antennas and other FPC antennas, the proposed array with ELP owns excellent merit of high gain. Because the ELP antenna element has preferable property of high gain and the PRS structure makes the gain be further enhanced, thus fewer numbers of elements can obtain the same effect as the arrays composed by traditional elements with large number.

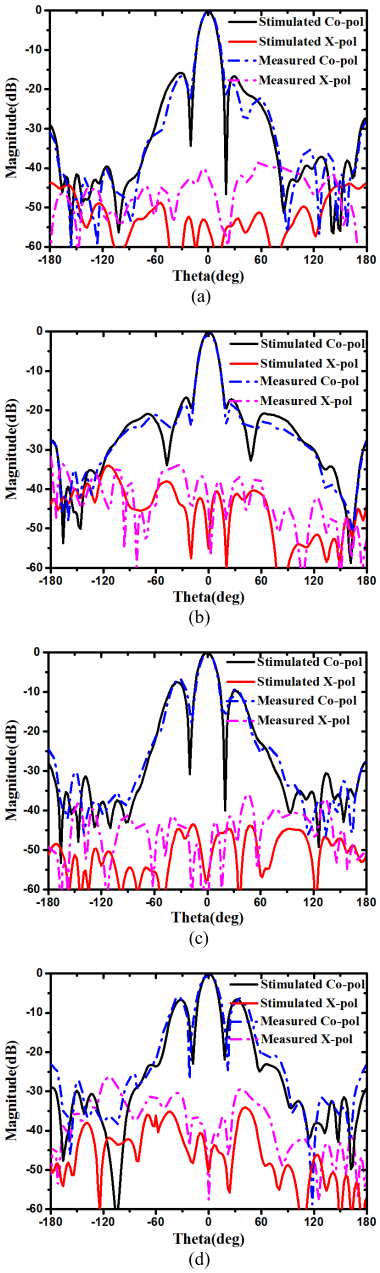

FIGURE 10. The measured and simulated radiation patterns of the fabricated 2 × 2 array at 21GHz. (a) E-plane with PRS, (b) H-plane with PRS, (c) E-plane without PRS, (d) H-plane without PRS.

What's more, for the ELP antenna array with fewer elements, the processing error caused by the complex structure can be reduced as well as the complexity and loss of the feeding network.

Additionally, compared with some methods to reduce grating lobes adopted in [4]–[8], this proposed strategy can avoid rely on the number of elements, the location of each elements and complex optimization algorithms such as genetic algorithms. What's more, compared with the using application limitation in [9], we can dramatically suppress the grating lobes of 2-D array with ELP under the premise of uniform arrangement of elements in this work. Meanwhile, this strategy can also be used to solve the grating lobes problem caused by large element spacing in other arrays.

IV. CONCLUSION

In this paper, a high gain and low grating lobe electrically large array antenna by using Fabry-Perot cavity is proposed. By introducing FPC structure, the beamwidth of ELP antenna can be effectively narrowed, thus the large grating lobes of ELP array caused by large element spacing can be avoided. This method overcomes the shortcomings of large number of elements and the complex location of elements under non-uniform arrangement. It provides a new way to solve the problem of grating lobes for 2-D larger spacing antenna arrays in the future.

REFERENCES

[1] W. Cao, B. Zhang, J. Jin, W. Zhong, and W. Hong, "Microstrip antenna with electrically large property based on metamaterial inclusions," *IEEE Trans. Antennas Propag.*, vol. 65, no. 6, pp. 2899–2905, Jun. 2017.
[2] W.-Q. Cao, W. Hong, and Y. Cai, "Microstrip-line-slot fed EDPA elements and array with ELP," *IET Microw. Antennas Propag.*, vol. 10, no. 12, pp. 1304–1311, Sep. 2016.
[3] Y. Cai, Z. Q. Qian, W. Q. Cao, Y. S. Zhang, and L. Yang, "Electrically large resonant cavity loaded with ε-negative and μ-negative metamaterials," *IEEE Antennas Wireless Propag. Lett.*, vol. 15, pp. 294–297, 2015.
[4] W. C. Barott and P. G. Steffes, "Grating lobe reduction in aperiodic linear arrays of physically large antennas," *IEEE Antennas Wireless Propag. Lett.*, vol. 8, pp. 406–408, 2008.
[5] Y. V. Krivosheev, A. V. Shishlov, and V. V. Denisenko, "Grating lobe suppression in aperiodic phased array antennas composed of periodic subarrays with large element spacing," *IEEE Trans. Antennas Propag.*, vol. 57, no. 1, pp. 76–85, Feb. 2015.
[6] Y. V. Krivosheev and A. V. Shishlov, "Grating lobe suppression in phased arrays composed of identical or similar subarrays," in *Proc. IEEE Int. Symp. Phased Array Syst. Technol.*, Waltham, MA, USA, Oct. 2010, pp. 724–730.
[7] S. Suarez, G. Leon, M. Arrebola, L. F. H. Ontanon, and F. L. H. Andres, "Experimental validation of linear aperiodic array for grating lobe suppression," *Prog. Electromagn. Res. C*, vol. 26, pp. 193–203, Jan. 2012.
[8] H. Wang, D.-G. Fang, and Y. L. Chow, "Grating lobe reduction in a phased array of limited scanning," *IEEE Trans. Antennas Propag.*, vol. 56, no. 6, pp. 1581–1586, Jun. 2008.
[9] Y. Zhang, W. Cao, Z. Qian, S. Shi, and W. Peng, "Low grating lobe array antenna with electrically large property based on TM_{50} mode," *IEEE Access*, vol. 7, pp. 32897–32906, 2019.
[10] J. R. Kelly and A. P. Feresidis, "Array antenna with increased element separation based on a Fabry–PÉrot resonant cavity with AMC walls," *IEEE Trans. Antennas Propag.*, vol. 57, no. 3, pp. 682–687, Mar. 2009.
[11] N. Wang, Q. Liu, C. Wu, L. Talbi, Q. Zeng, and J. Xu, "Wideband Fabry-Perot resonator antenna with two complementary FSS layers," *IEEE Trans. Antennas Propag.*, vol. 62, no. 5, pp. 2463–2471, May 2014.
[12] R. Lian, Z. Tang, and Y. Yin, "Design of a broadband polarization-reconfigurable Fabry–Pérot resonator antenna," *IEEE Antennas Wireless Propag. Lett.*, vol. 17, no. 1, pp. 122–125, Jan. 2018.
[13] Z.-G. Liu and W.-B. Lu, "Low-profile design of broadband high gain circularly polarized Fabry–Pérot resonator antenna and its array with linearly polarized feed," *IEEE Access*, vol. 5, pp. 7164–7172, 2017.
[14] W. Cao, X. Lv, Q. Wang, Y. Zhao, and X. Yang, "Wideband circularly polarized Fabry–Pérot resonator antenna in Ku-band," *IEEE Antennas Wireless Propag. Lett.*, vol. 18, no. 4, pp. 586–590, Apr. 2019.
[15] Z.-H. Wu and W.-X. Zhang, "Broadband printed compound air-fed array antennas," *IEEE Antennas Wireless Propag. Lett.*, vol. 9, pp. 187–190, 2010.
[16] H. Attia, M. L. Abdelghani, and T. A. Denidni, "Wideband and high-gain millimeter-wave antenna based on FSS Fabry–Pérot cavity," *IEEE Trans. Antennas Propag.*, vol. 65, no. 10, pp. 5589–5594, Oct. 2017.
[17] Y. Sun, Z. N. Chen, Y. Zhang, H. Chen, and T. S. P. See, "Subwavelength substrate-integrated Fabry-Pérot cavity antennas using artificial magnetic conductor," *IEEE Trans. Antennas Propag.*, vol. 60, no. 1, pp. 30–35, Jan. 2012.

[18] A. R. Vaidya, R. K. Gupta, S. K. Mishra, and J. Mukherjee, "Right-hand/left-hand circularly polarized high-gain antennas using partially reflective surfaces," *IEEE Antennas Wireless Propag. Lett.*, vol. 13, pp. 431–434, 2014.
[19] H. Jin, W. Che, K.-S. Chin, W. Yang, and Q. Xue, "Millimeter-wave TE_{20}-mode SIW dual-slot-fed patch antenna array with a compact differential feeding network," *IEEE Trans. Antennas Progag.*, vol. 66, no. 1, pp. 456–461, Jan. 2018.
[20] T. Y. Yang, W. Hong, and Y. Zhang, "Wideband millimeter-wave substrate integrated waveguide cavity-backed rectangular patch antenna," *IEEE Antennas Wireless Propag. Lett.*, vol. 13, pp. 205–208, 2014.
[21] X. Zhang, L. Zhu, and Q. Wu, "Sidelobe-reduced and gain-enhanced square patch antennas with adjustable beamwidth under TM_{03} mode operation," *IEEE Trans. Antennas Propag.*, vol. 66, no. 4, pp. 1704–1713, Apr. 2018.
[22] C. A. Balanis, *Antenna Theory: Analysis and Design*. Hoboken, NJ, USA: Wiley, 2005.

YUNYANG ZHANG received the B.S. degree in electronic science and technology from Inner Mongolia University, Hohhot, China, in 2017. He is currently pursuing the M.S. degree with the College of Communication Engineering, Army Engineering University of PLA, Nanjing, China. His current research interests include millimeter-wave antennas, array antenna technology with electrically large property, and their applications to microwave components and antennas.

WENQUAN CAO received the B.S. and Ph.D. degrees from the Institute of Communications Engineering, Nanjing, China, in 2008 and 2014, respectively. He is currently an Associate Professor with the College of Communications Engineering. He has authored and coauthored more than 100 conference and journal papers, including more than 30 in IEEE periodicals. His current research interests include microstrip antennas, metamaterials, and their applications to microwave components and antennas. He is currently serving as a Reviewer for the IEEE TRANSACTIONS ON MICROWAVE THEORY AND TECHNIQUES, the IEEE MICROWAVE AND WIRELESS COMPONENTS LETTERS, the IEEE ANTENNAS AND WIRELESS PROPAGATION LETTER, and IEEE ACCESS.

ZUPING QIAN was born in Haimen, Jiangsu, China, in 1961. He received the B.S. and M.S. degrees in applied mathematics from Hunan University, Changsha, China, in 1982 and 1985, respectively, and the Ph.D. degree in microwave techniques from Southeast University, Nanjing, China, in 2000. From 1985 to 1999, he was with the Institute of Communications Engineering, Nanjing, as a Lecturer and later as an Associate Professor. Since 2000, he has been a Professor with the College of Communications Engineering, PLA University of Science and Technology, Nanjing. He authored several books, such as *Electromagnetic Compatibility, Antenna, and Propagation*. He has authored over 80 international and regional refereed journal papers. His research interests include antenna, metamaterials, computational electromagnetics, array signal processing, and EMI/EMC.

TING PAN received the B.S. degree in information and computing science from the Wuhan University of Science and Technology, in 2017. She is currently pursuing the M.S. degree with the College of Communication Engineering, Army Engineering University of PLA, Nanjing, China. Her research interests include communication technology, data mining, and machine learning.